IMPROVEMENT IN PERFORMANCE OF WIRELESS RELAY NODES USING PHYSICAL LAYER NETWORK CODING

A Thesis

by

NAGA RAGHAVENDRA ANUDEEP TUNGALA

Submitted to the Office of Graduate and Professional Studies of
Texas A&M University
in partial fulfillment of the requirements for the degree of

MASTER OF SCIENCE

Chair of Committee,	Scott L. Miller
Committee Members,	Krishna Narayanan
	Alex Sprintson
	Andreas Klappenecker
Head of Department,	Miroslav Begovic

December 2015

Major Subject: Electrical Engineering

ABSTRACT

Recent advancements in high data rate networks have led to a growing interest in improving performance of wireless relay networks through the use of Physical Layer Network Coding (PLNC) technique. In the PLNC technique, the relay node exploits the network coding operation that occurs naturally when the two electromagnetic (EM) waves are superimposed on one another to directly decode the modulo-2 sum of the transmitted symbols.

In this thesis, we will present an optimal power control algorithm for performance improvement in wireless relay nodes implementing physical layer network coding. We shall also present a sub-optimal power control algorithm and compare its performance with the optimal power control algorithm. Our approach will first derive the probability of error for the amplitude-controlled system using Maximum Likelihood detection and then minimize the probability of error using amplitude control functions as variables to derive the optimal power control functions. We shall start by considering the thresholds of the system to be the maximum of the independent received amplitudes to derive the probability of error equations and then extend it to a variable threshold system, where the threshold is a function of independent received amplitudes. We then derive an optimal power control algorithm for a single channel Rayleigh system and implement this power control algorithm independently on the terminals to achieve a sub-optimal power control algorithm.

Our results show that the proposed optimal power control algorithm boosts the performance of the PLNC system significantly compared to the no power control system. We also show that there are no significant differences between the performances of optimal power control and the sub-optimal power control algorithms. We further

show that the performance of the system is not degraded much when the amplitudes of the terminals deviate from the optimal amplitudes.

DEDICATION

To my family, friends and professors

ACKNOWLEDGEMENTS

First and foremost, I would like to express my sincere gratitude to my advisor Dr. Scott Miller for introducing me to research and being so patient and supportive, especially in the tough times. The detailed feedback from him on my results and progress helped me significantly during this work. This thesis would not have been possible without his guidance and support. I would also like to thank the members of my advisory committee for the intriguing questions and suggestions about my work. Thanks to the staff in the Department of Electrical Engineering for making my academic life here so convenient and to faculty for providing me with the important knowledge needed for research. I am also thankful to my parents, Usha Rani and SreeRama Murthy without whom I would not have been able to accomplish this task. A special thanks to my friends Mallikarjun Rao Kanala, members of TAMU Jeffas and Wipro gang for their support and encouragement which made this work possible.

TABLE OF CONTENTS

Page

LIST OF FIGURES

FIGURE Page

LIST OF TABLES

TABLE Page

1. INTRODUCTION

As the demand for high data rate systems increases, there is a surge in the deployment of wireless relay networks for data communications. A relay network is a broad class of network topology commonly used in wireless networks, where the source and destination cannot directly communicate with each other, because either their distance of separation does not match the individual range due to high data rates or, due to obstacles in the path of communication. As the data rate increases the receiver sensitivity decreases with an increase in range. So to attain better performance while transmitting high data rates, wireless relay network topology is being used for such communications. Throughput and performance are the major factors to be considered for any communication system. In order to improve the throughput efficiency of relay networks, a few techniques were introduced in [15],[18],[5],[4]. Among the various throughput improvement techniques, Physical Layer Network Coding stands out. In this section, we provide a brief overview of PLNC and how it is better compared to other techniques. We also present the scenarios and assumptions considered in this thesis.

1.1 Physical Layer Network Coding

Let us consider a simple relay network as shown in Figure 1.1. This simple relay network, which comprises of two transmitters communicating with each other via a relay node, can be extended to a multi-hop network. Similarly, the performance and throughput improvement achieved on each individual hop can improve overall system performance and throughput. The standard way of transmission in this simple relay node takes a total of four time slots for complete two way communication as shown in Figure 1.2. Communication between the nodes happens in different time slots to

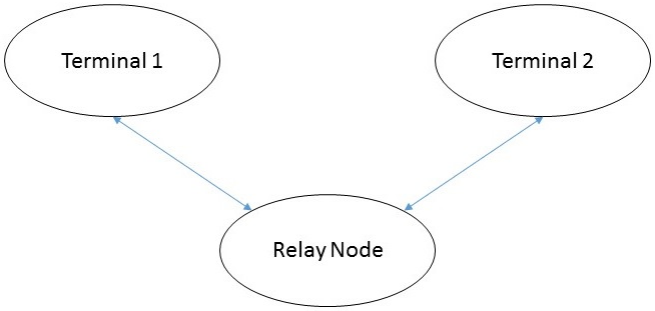

Figure 1.1: Basic wireless relay node

prevent interference of the signals. The relay receiver will be of minimum complexity for this standard transmission.

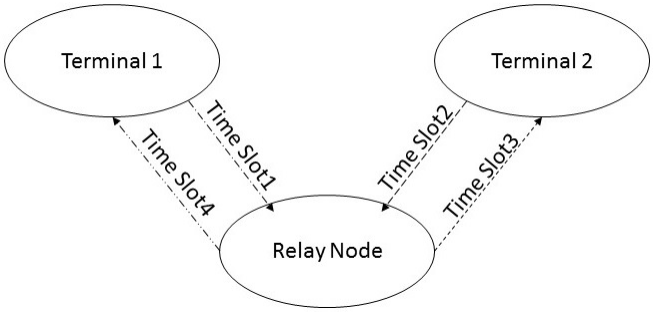

Figure 1.2: Standard transmission in wireless relay nodes

Relay networks that employ network coding concepts achieve better performance compared to the standard techniques. Network coding refers to a scheme where a node is allowed to generate output data by mixing (i.e., computing certain functions of) its received data. Digital Network Coding (DNC) and Physical Layer Network Coding (PLNC) are the two main techniques in network coding. In the DNC technique, as shown in Figure 1.3, the two terminals transmit data to the relay node in two different time slots. The relay decodes the received symbols independently, then

computes the modulo-2 sum of them in a symbol by symbol manner. The modulo-2 sum/ Xored symbol sequence is then broadcast back to the terminals in the third time slot. Now, the terminals can decode the symbols transmitted by the other terminal by performing a modulo-2 sum of the received broadcast sequence from the relay and their own buffered transmitted symbol sequence. Thus, DNC requires three time slots to complete a round of data exchange between terminals.

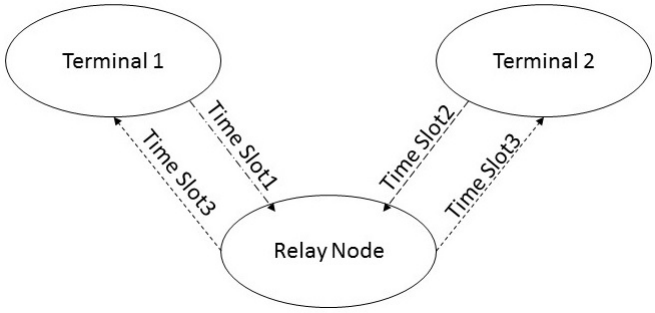

Figure 1.3: DNC technique

In the PLNC technique, as shown in Figure 1.4, the two terminals transmit data simultaneously to the relay node. The relay node then exploits the network coding operation that occurs naturally when electromagnetic (EM) waves are superimposed on one another, to directly decode the modulo-2 sum of the transmitted symbols from the two terminals. In the next time slot, the relay node broadcasts back the decoded modulo-2 sum back to the terminals, which perform a similar process as in DNC to recover data transmitted by the other terminal. Thus, the PLNC technique requires only two time slots to complete a round of data exchange between the terminals, achieving a throughput improvement over the DNC technique. This throughput improvement over DNC comes at the cost of additional receiver complexity.

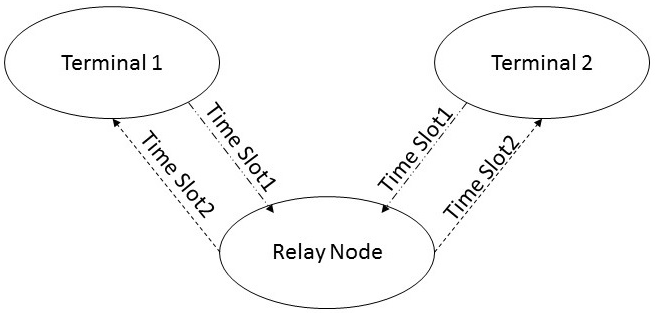

Figure 1.4: PLNC technique

1.2 Assumptions and Scenarios

In this work, we assume the relay network to divide the time into fixed time slots and data is transmitted in packets that will fit into a given time slot. Each data packet consists of a preamble followed by the information carrying data bits. The preamble is set of bits known to the both transmitter and the receiver whereas the data bits are known to the transmitter but not to the receiver. These bits in the preamble facilitate coherent detection of the signal by assisting in continuous estimation of channel parameters as proposed in [3]. These estimated channel parameters are communicated to the transmitters as overhead over in the packets broadcast from the relay node. Assuming a slow varying channel, the transmitters will have the estimates of the present channel parameters. The major contribution of this thesis is to take advantage of this complex continuous tracking and estimation of channel parameters and design power control techniques over PLNC to achieve performance improvement in relay networks.

In order to support the assumptions made in this work, consider a scenario in which the terminals, T_1 and T_2 are communicating through a relay node, R using QPSK modulation. Continuous tracking and estimation of channel parameters helps

in coherent detection of these modulations at the receiver. The phase synchronized signal constellations for QPSK modulation, achieved through channel parameter estimation can be considered as two independent BPSK modulations over I and Q channels. So, in this thesis work, we assume a simple relay network using the PLNC technique which communicates with an underlying BPSK modulation format. The power control algorithms derived for the optimal performance of BPSK modulation can be extended to QPSK, leveraging the above discussed fact.

1.3 Outline of Thesis

This thesis contains three more sections. In section 2, we briefly provide the background necessary to understand this thesis. We also provide a discussion of related work. In section 3, we propose our power control algorithms to achieve the optimal performance on the wireless relay networks along with the simulation results. We also compare the proposed algorithms with each other. Conclusions and future work possibilities are discussed in section 4.

2. BACKGROUND AND RELATED WORK

2.1 Background

Before delving into the thesis, let us review some background and related work which will prove essential for better understanding of thesis.

2.1.1 Communication on Wireless Channels

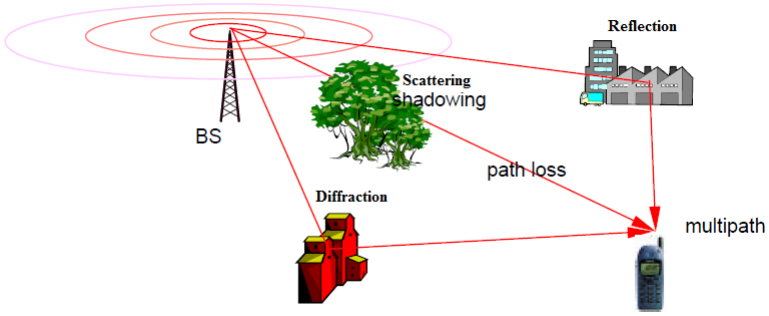

Figure 2.1: Multipath propagation

Communications over wireless channels follow the multipath propagation model as shown in Figure 2.1. Apart from the direct line of sight propagation, the signals from the transmitter bounce off various objects before reaching the receiver. The signals emanating from the transmitter does not propagate in the direction of the receiver alone. Even when the directional antenna is used, the signal propagates over a range of angles. As a result, the transmitted signals spread from the point of origin and will reach other objects like hills, buildings, trees and gets reflected off from the surfaces before reaching the receiver. Thus the signals bounces off from different surfaces and reach the receiving antenna via paths other than the direct line of sight.

All the multipath signals from the transmitter sums to the overall received signal at the receiver. Sometimes the multipath signals will be in phase or out of phase with the main signal. The in phase signal components will be added to the main signal increasing the signal strength and some times these components will interfere with each other, resulting in the overall signal strength reduction. The relative movements between the transmitter and the receiver can result in changes in the relative path lengths of the different multipath signals. This phenomenon is called fading and is present on many signals received on wireless channels. The fading is mainly of two types, flat fading and frequency selective fading. In flat fading all frequencies have equal attenuation across a given channel and frequency selective fading , which means different frequencies experience different fading levels.

2.1.2 Synchronization and Its Importance in PLNC

As we have seen in the previous section, the attention given to PLNC based relay-aided communications is due to its ability to improve throughput of the system. Synchronization of the received signals at the relay is a roadblock issue for the practical implementation of PLNC. There are three levels of synchronization assumed in PLNC in [18], namely symbol-level time synchronization, carrier-frequency synchronization and carrier-phase synchronization. The imperfect synchronization at the relay can have detrimental effects on the performance of PLNC as discussed in [19].

Let us consider the PLNC model system as shown in Figure 1.4, where two terminals exchange data via a relay node using BPSK modulation. As proposed in [19], the two received signals can be written as:

$$s_1(t) = a_1 cos(2\pi f t)$$

$$s_2(t) = a_2 cos(2\pi ft + \theta)$$

where a_1 and a_2 are the information bits, $\theta \quad (\frac{-\pi}{2} \leq \theta < \frac{\pi}{2})$ is the phase offset between the two received signals (this was assumed to be known at the receiver) and f is the carrier frequency. The power penalty for the phase error was given as

$$\Delta\gamma(\theta) = cos^2(\frac{\theta}{2}).$$

From the above equation, the worst case penalty for imperfect carrier-phase synchronization can be 3dB for a BPSK modulation and 6 dB for QPSK modulation. With the carrier frequency synchronization errors, we get a power penalty of 0.6dB. Similarly with the symbol time synchronization errors we get a penalty of almost 1.57dB. Overall it was concluded in [19] that imperfect synchronization at the relay results in performance degradation of 1 to 3 dB for systems using BPSK modulation. This penalty can be at higher levels for higher modulation formats. The symbol-level time synchronization to an extent is also important to prevent substantial performance loss in PLNC as proposed in [9]

Most of the research regarding PLNC focused on the two main aspects: asynchronous PLNC [6],[8], [17] and synchronous PLNC [11], [16], [13], [14], [10]. The basic idea in asynchronous PLNC is to map the superposed signal with arbitrary phase differences to encoded symbols. The channel state information is necessary to estimate these instantaneous phases of the signals superposing at the relay. In the synchronous case, it is assumed that the channel state information is known at the relay and the signals arrive in phase at the relay.

Overall, both the synchronous and asynchronous methods need to estimate and track the instantaneous channel parameters continuously to facilitate the practical

implementation of PLNC.

2.1.3 Channel Parameter Estimation and Tracking

Estimating the channel parameters and tracking them continuously is a complex process. This can be implemented either by blind estimation at the relay [20], [1] or by using the known preamble as overhead over packets [3]. The estimated channel parameters are made available to the terminals as overhead over the broadcast packets from the relay node. These complex parameters are quantized at the relay before being broadcast to the terminals. The quality of the recovered channel information at the terminals depends on the number of quantization bits. In the literature some of the works such as [12] assume that the forward channel link, between the terminal and the relay, is similar to the reverse channel link, between the relay and terminal, so that both the links have same channel parameters. If this is the case there is no requirement to transmit the channel parameters back to the terminals. We can leverage this complex estimation of channel information to further improve the performance at the relay by using the estimated channel parameters to control the power of the transmitted symbols to achieve optimal performance at the relay by minimizing the instantaneous BER. There has been a lot of research done in single channel power control, especially for CDMA where the near-far effects of users are to be minimized by adjusting their transmit powers so that the signals at the receiver are at equal amplitudes or power. The major work in this thesis is to derive the optimal power control algorithms in PLNC and show how the well settled phenomenon of equal received amplitudes at the relay from terminals does not apply in the PLNC case for optimal performance.

2.2 Previous Work

The application of power control techniques over two way relay channels using PLNC has seen many techniques providing substantial improvement in performance at the relay node.

2.2.1 Power Control for PLNC in Fading Environments

In this section, we will discuss the power control strategies proposed in [12]. In this paper, the average BER at the terminals in Two Way Relay Network was analyzed as the sum of the BER at the relay and the BER at the terminals. The signal constellation mapping at the relay is as shown in Figure 2.2. It is assumed for illustration purposes that the channel parameters are known at the relay and $|h_1| > |h_2|$.

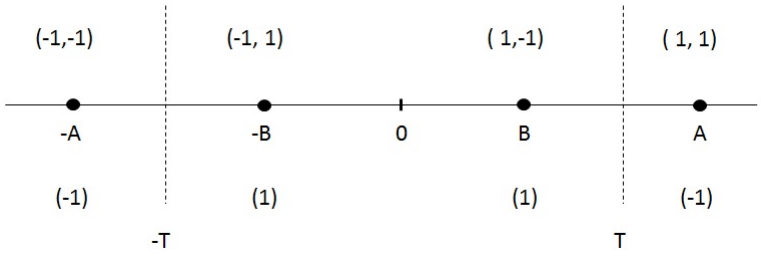

Figure 2.2: Signal constellation of received signal at the relay node

A and B are mapped signal constellation points at the relay, where

$$A = ||h_1|\sqrt{R_1} + |h_2|\sqrt{R_2}|$$

$$B = ||h_1|\sqrt{R_1} - |h_2|\sqrt{R_2}|$$

where R_1 and R_2 are the controlled symbol powers. The received signal at the relay is given by

$$R_x = h_1\sqrt{R_1}S_1(n) + h_2\sqrt{R_2}S_2(n) + n(t) \tag{2.1}$$

where $S_1(n)$ and $S_2(n) \in \{\pm 1\}$ are the transmitted symbols from the terminals. At higher SNRs where both A and B are greater than $3\sigma_n^2$, the value of the threshold T will approach $\frac{A+B}{2}$. Using $T = \frac{A+B}{2}$ as the decision boundary, the average BER caused by PLNC mapping is

$$P(error|h1, h2) = Q(\lambda_{min}) + \frac{1}{2}Q(2\lambda_{max} - \lambda_{min}) - \frac{1}{2}Q(2\lambda_{max} + \lambda_{min}) \tag{2.2}$$

where

$$\lambda_{min} = min(|h_1|\sqrt{\frac{2R_1}{N_0}}, |h_2|\sqrt{\frac{2R_2}{N_0}})$$

$$\lambda_{max} = max(|h_1|\sqrt{\frac{2R_1}{N_0}}, |h_2|\sqrt{\frac{2R_2}{N_0}})$$

The probability of error mentioned in the previous equation was approximated with only the dominant Q-function term because

$$Q(\lambda_{min}) > \frac{1}{2}[Q(2\lambda_{max} - \lambda_{min}) - Q(2\lambda_{max} + \lambda_{min})]$$

thereby

$$P(error|h_1, h_2) \cong Q(\lambda_{min}) \tag{2.3}$$

The probability of error estimated was minimized to derive the power control functions on terminals that can improve the performance of the system. The overall transmit energy from the terminals is constrained to some value, 2ε to prevent

consideration of infinite powers at the terminals,

$$min \quad P(error|h1, h2),$$

$$subject \quad to \quad \frac{R_1 + R_2}{2} = 2\overline{\varepsilon}.$$

Since the Q-function is a monotonically decreasing function, minimizing a Q function with respect to the constraints is equivalent to maximizing the argument. By considering the above fact and with respect to constraints, the equation that should be maximized is

$$min(|h_1|\sqrt{\frac{2R_1}{N_0}}, |h_2|\sqrt{\frac{2R_2}{N_0}})$$

This maximization is assumed to occur when

$$|h_1\sqrt{R_1}| = |h_2\sqrt{R_2}|$$

Solving the above minimization problem, the equations for R_1 and R_2 were derived to be

$$R_1 = \frac{2|h_2|^2\varepsilon}{|h_1|^2 + |h_2|^2}, \tag{2.4}$$

$$R_2 = \frac{2|h_1|^2\varepsilon}{|h_1|^2 + |h_2|^2}. \tag{2.5}$$

The probability of error curve for the system model and the performance improvement by implementing the above mentioned power control algorithm at the terminals is as shown in the Figure 2.3. The power control function graph with respect to the co-channel gain of 0.5 at 3dB for the system is as shown in Figure 2.4.

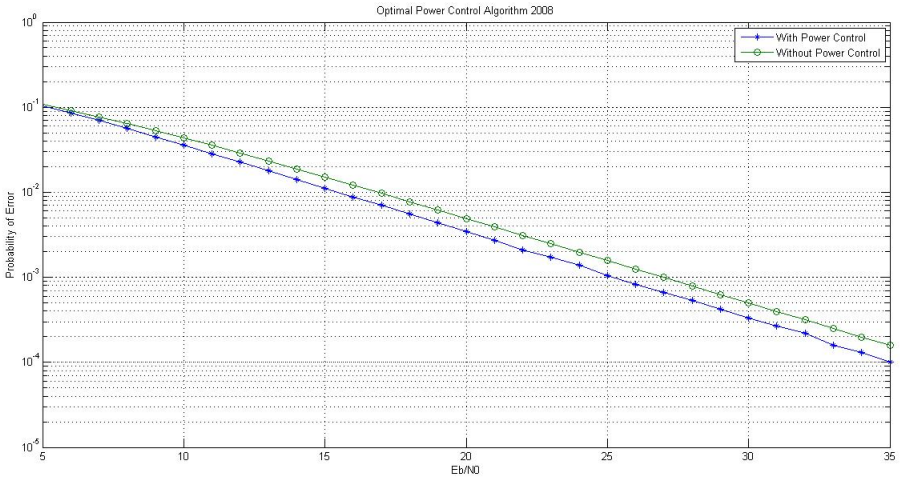

Figure 2.3: Performance improvement for power control algorithm 2008

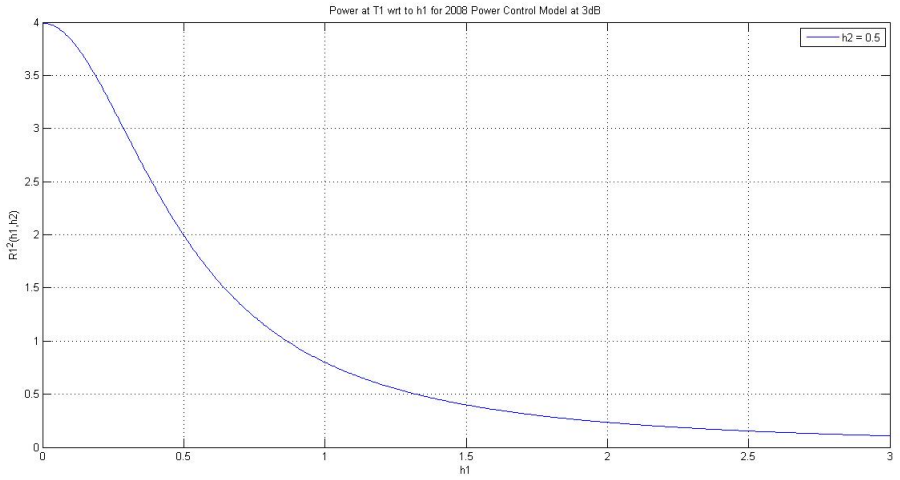

Figure 2.4: Power control function wrt H for 2008 power control algorithm

2.2.2 Power Control Using Channel Parameters Ratio

In this section we will discuss the limited feedback quantization power control method proposed in [7]. The system model is similar to the two way relay network

PLNC model shown in Figure 1.4. The system is assumed to have channel state information known at the relay node. The received signal at the relay is taken as,

$$R_x = h_1\sqrt{R_1}S_1(n) + h_2\sqrt{R_2}S_2(n) + n(t) \tag{2.6}$$

where R_x is the received amplitude at the relay, h_1 and h_2 are the channel parameters of terminal 1 and terminal 2 respectively, $S_1(n), S_2(n) \in \Omega$, where Ω is the modulation constellation alphabet and $n(t)$ is the complex additive white Gaussian noise with variance σ^2.

The transmission power is constrained and is made to be below some value R^{max} on each of the terminals. Without any power control, the terminals will be transmitting symbols at some R^{min}, which is the minimum transmitting power required to achieve the required data rate. The denoising function

$$(\hat{S_1}, \hat{S_2}) = arg \min_{(S_1(n),S_2(n))\in\Omega\times\Omega} |R_x - \sqrt{R_1}h_1S_1(n) - \sqrt{R_2}h_2S_2(n)|^2 \tag{2.7}$$

is used for XOR mapping of the received signal at the relay to perform the PLNC. The optimal power scheme is taken at the condition where

$$|h_1|^2R_1 = |h_2|^2R_2$$

$$subject \quad to \quad R_1 \leq R_{max}, R_2 \leq R_{max}$$

The quantity β, is defined as the modified ratio of $|h_1|^2$ to $|h_2|^2$,

$$\beta = \begin{cases} \frac{|h_1|^2}{|h_2|^2} & for \quad |h_1|^2 > |h_2|^2, \\ \frac{|h_2|^2}{|h_1|^2} & for \quad |h_2|^1 > |h_1|^2. \end{cases}$$

$$for \quad \beta \in [1, +\infty)$$

This β is transmitted back to the terminals where they modify their instantaneous transmit power as a function of β. The terminal with a good channel compared to the other will reduce its power as a function of the modified ratio β and the terminal with the bad channel transmits the minimum required power to achieve the required data rate.

$$If \quad |h_2| > |h_1| \quad R_1 = R_1^{min} < R_1^{max}, \quad R_2 = \frac{R_1^{min}}{\beta} < R_2^{max}$$

$$If \quad |h_1| > |h_2| \quad R_1 = \frac{R_2^{min}}{\beta} < R_1^{max}, \quad R_2 = R_2^{min} < R_2^{max},$$

The probability of error curve for the system model and the performance improvement by implementing the above mentioned power control algorithm at the terminals is as shown in the Figure 2.5. The power control function graph with respect to the co-channel gain of 0.5 at 3dB for the system is as shown in Figure 2.6.

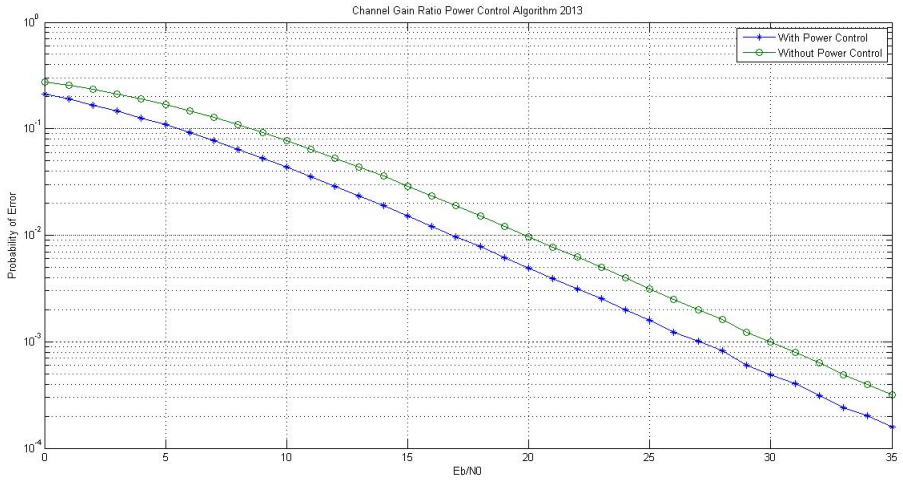

Figure 2.5: Performance improvement for power control algorithm 2013

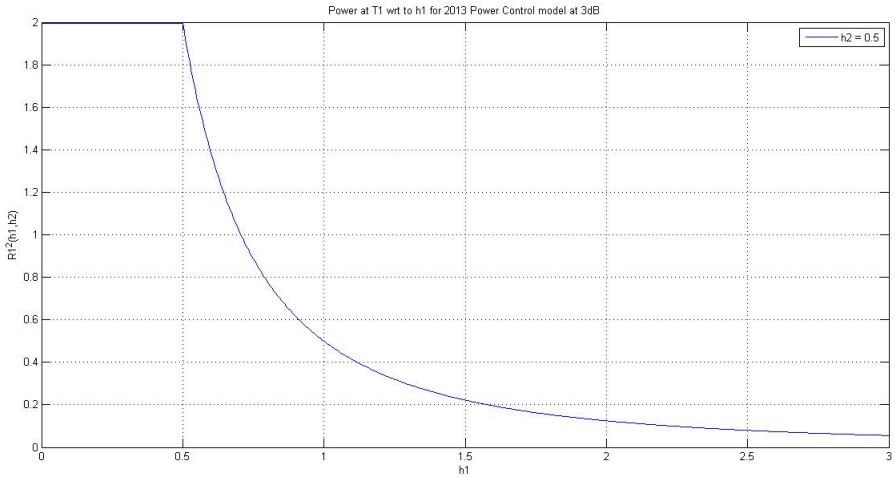

Figure 2.6: Power control function wrt H for power ratio algorithm

2.2.3 Adaptive Feedback Communications

In this section, we will discuss the adaptive feedback communication methods for a single user system, proposed in [2]. The system envisions an adaptive receiver and a feedback channel as shown in Figure 2.7. The feedback channel conveys information to the transmitter on the forward channel state learned at the receiver. The transmitter uses this information to modify the transmit power of the underlying BPSK modulation symbols.

The adaptive power control scheme for coherent detection at the receiver discussed in this paper stands as a main motivation for our thesis work. Let us provide a qualitative analysis of the approach followed in this paper to find the optimal power control function for this single user case. This analysis helps in better understanding our minimization technique which is extended to the two user PLNC case.

The probability of error for the system as shown in Figure 2.7, at the relay was

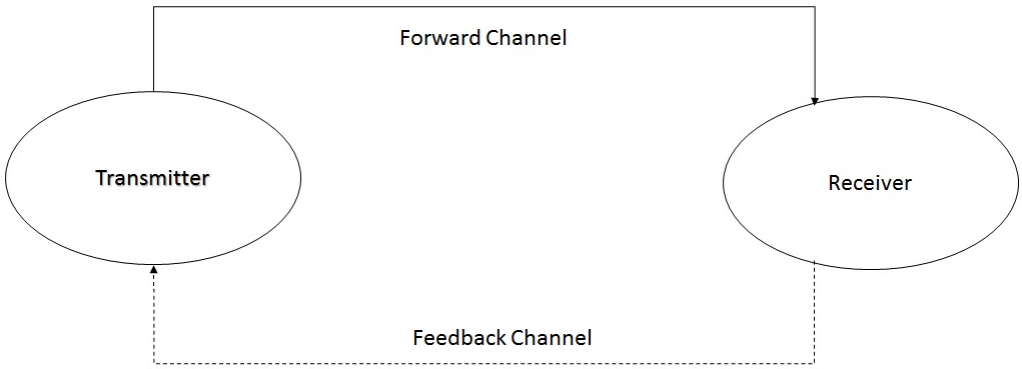

Figure 2.7: Single user system

given as

$$P(error|h) = Q(|h|\sqrt{2R(h)}) \tag{2.8}$$

where $|h|$ is the channel gain known at the relay, $R(h)$ is the BPSK symbol power as a function of feedback channel information. The average Probability of error was minimized with a constrained minimization function, where

$$\int R^2(h) * f(h) * dh = M$$

is the constraint over minimizing the probability of error. This minimization was carried out using Lagrange minimization technique, where minimization was performed on each instantaneous minimization function

$$Q(|h|\sqrt{2R(h)}) + \mu R(h)$$

with $R(h)$ as a variable.

Thus we arrive at a closed form equation for R which is an optimal amplitude con-

trol function at the transmitter to minimize the BER at relay based on the available channel parameters.

The probability of error curve for the system model and the performance improvement by implementing the above mentioned power control algorithm at the terminal for single channel case is as shown in the Figure 2.8. The power control function graph with respect to the co-channel gain of 0.5 at 3dB for the system is as shown in Figure 2.9.

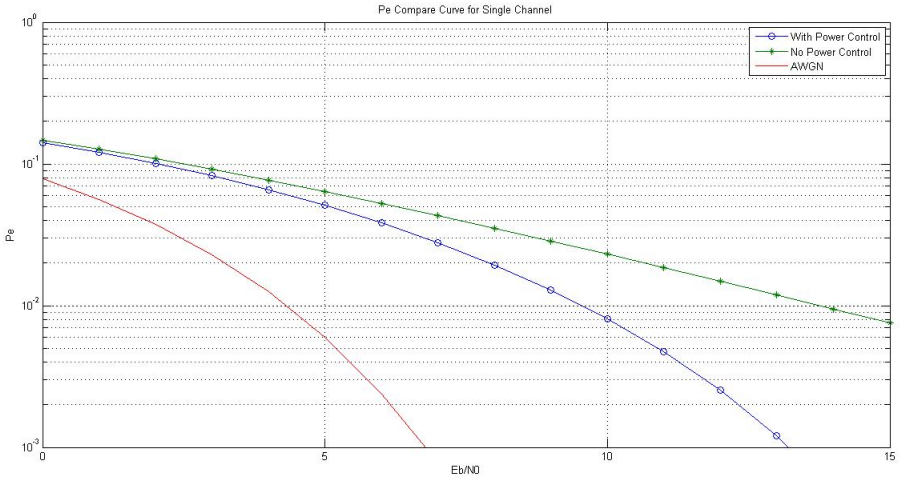

Figure 2.8: Performance improvement for power control algorithm in single user case

2.3 Goals and Motivation

As discussed in the previous section most of the optimization techniques for TWRN implementing PLNC assumed that the optimal power control occurs at $|h_1|R_1 = |h_2|R_2$. In this thesis work,

- We propose optimal power control algorithms that proves the well settled assumption of $|h_1|R_1 = |h_2|R_2$ at the relay is wrong in deriving optimal power

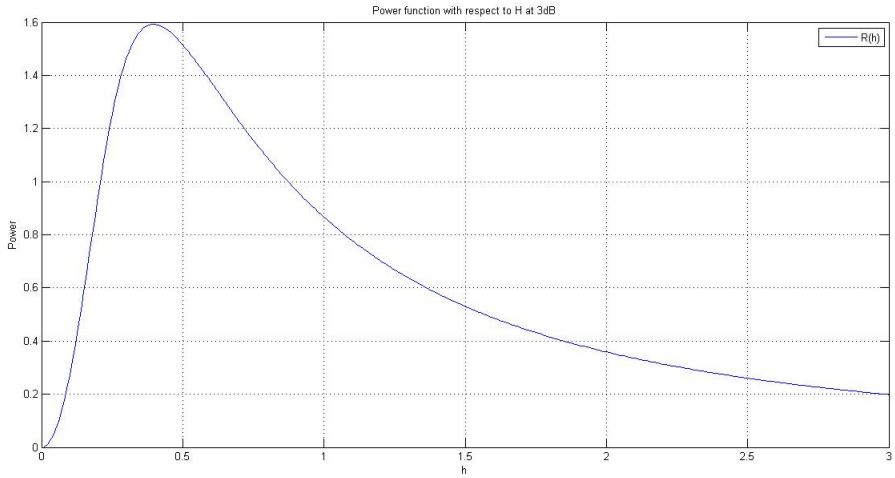

Figure 2.9: Power control function wrt H at 3dB for single user case

control algorithms.

- We propose an optimal co-channel dependent power control algorithm, where the instantaneous transmit symbol power at a terminal is a function of its channel state information and the co-channel or the other terminals channel state information. This algorithm achieves better performance at the relay compared to the existing algorithms.

- We also propose an optimal co-channel independent algorithm that achieves performance similar to the above mentioned co-channel dependent power control algorithm.

- From the co-channel independent algorithm's performance we also propose that the co-channel information is not necessary at the terminal to achieve the optimal performance.

3. OPTIMAL POWER CONTROL ALGORITHMS

We put forth the optimal power control algorithms in this section. In the first section we describe our system model. A detailed study of algorithms is carried out in the second section. Simulation results for each algorithm are also presented in this section.

3.1 System Model

A wireless relay network with two terminals T_1 and T_2 exchanging information via a relay node is our system model. The wireless channel between the terminals and the relay is assumed to be a slow varying Rayleigh fading channel. The terminals are assumed to have the knowledge of channel parameters for the transmitting frame in the given time slot. Let us assume h_1 as the channel gain between the Terminal 1 and the relay node, h_2 as the channel gain between the Terminal 2 and the relay node. Let us also assume $A_1(h_1, h_2)$ as the input symbol amplitude from Terminal 1 and $A_2(h_1, h_2)$ as the input symbol amplitude from Terminal 2. They are denoted as A_1 and A_2 for simplicity.

With the absence of white noise at the relay the general signal constellation at the relay for given inputs is as shown in the Table 3.1:

Table 3.1: Signal constellations at relay without white noise

Normal Input Data	Antipodal form	Constellation at Rx	XOR mapped
(1,1)	(+1,+1)	$h_1A_1 + h_2A_2$	0
(1,0)	(+1,-1)	$h_1A_1 - h_2A_2$	1
(0,1)	(-1,+1)	$-h_1A_1 + h_2A_2$	1
(0,0)	(-1,-1)	$-h_1A_1 - h_2A_2$	0

Graphical representation for the signal constellations as shown in Table 3.1, can be depicted in 2 different ways as the threshold in between the constellation points depends on the received symbol amplitudes whether $h_1A_1 > h_2A_2$ or $h_1A_1 < h_2A_2$. Therefore the general representation of the signal constellation and the probability of error is divided into two cases as shown in the Figures 3.1 and 3.2.

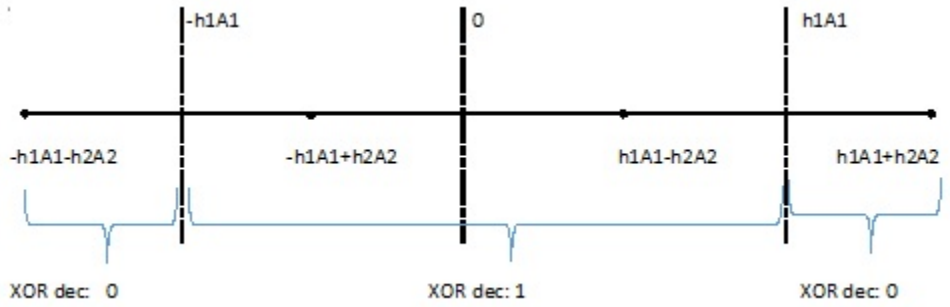

Figure 3.1: Case 1: $h_1A_1 > h_2A_2$

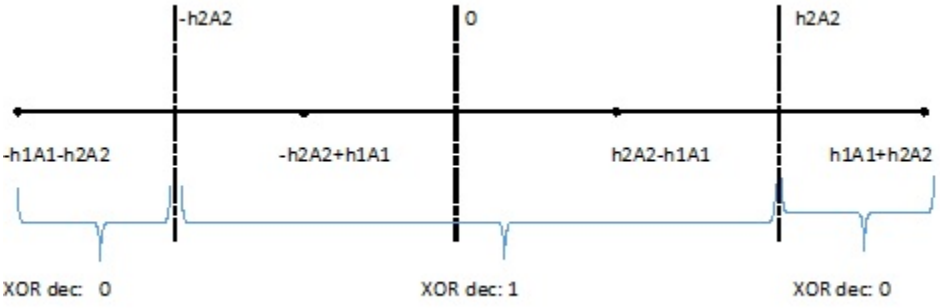

Figure 3.2: Case 2: $h_1A_1 < h_2A_2$

An error occurs at the relay if the decoded symbol does not match the actual transmitted symbol as mentioned in Table 3.1. The channel distortions and the Ad-

ditive White Gaussian Noise (AWGN) contributes to the errors at the relay receiver. Let R_x be the received amplitude at the relay, which is a combination of individual amplitudes multiplied with their respective channel gains and AWGN. As the probability of error depends on the thresholds that separate the symbols in a signal constellation, the probability of error for the system is divided into two different cases.

3.2 Probability of Error

The probability of error for our system at the relay in general is given as

$$P(error|h_1,h_2) = P(error|h_1,h_2,1sent)*P(1sent)+P(error|h_1,h_2,0sent)*P(0sent) \tag{3.1}$$

where the '1' and '0' sent are the xor combination of the transmitted symbols from the terminals. Since the probability of sending a '1' or '0' from the terminals is equally likely, we can consider

$$P(error|1sent) = P(error|0sent) = \frac{1}{2}$$

So the probability of error for the given case becomes

$$\begin{aligned} P(error|(h_1,h_2)) = \frac{1}{2}[&P(error|(h_1,h_2,1sent)) \\ &+ P(error|(h_1,h_2,0sent))] \end{aligned} \tag{3.2}$$

where "1 sent" and "0 sent" are the superimposed XOR symbols resulted from the simultaneous transmission of data symbols from the terminals 1 and 2.

3.2.1 Probability of Error with Fixed Threshold

Let us first consider Case 1 where $h_1A_1 > h_2A_2$. As R_x is the received amplitude at the relay, from Figure 3.1, equation 3.2 can be written as follows

$$P(error|h_1,h_2) = \frac{1}{2} * [P(R_x < -h_1A_1 \cup R_x > h_1A_1)|1sent) + P(R_x > -h_1A_1 \cap R_x < h_1A_1)|0sent)] \quad (3.3)$$

Solving each of the terms in equation 3.3 independently, the first term:

$$P(error|1sent) = Q(\frac{2h_1A_1 - h_2A_2}{\sigma_N}) + Q(\frac{h_2A_2}{\sigma_N}) \quad (3.4)$$

Now considering the second term of the equation 3.3 i.e

$$P(error|0sent) = Q(\frac{h_2A_2}{\sigma_N}) - Q(\frac{2h_1A_1 + h_2A_2}{\sigma_N}) \quad (3.5)$$

Substituting equations 3.4 and 3.5 in the equation 3.3 gives us

$$P(error|h_1,h_2) = Q(\frac{h_2A_2}{\sigma_N}) + \frac{1}{2}[Q(\frac{2h_1A_1 - h_2A_2}{\sigma_N}) - Q(\frac{2h_1A_1 + h_2A_2}{\sigma_N})] \quad (3.6)$$

$$[h_1A_1 > h_2A_2]$$

Now let us consider Case 2, where $h_1A_1 < h_2A_2$. So, the threshold for the system is h_2A_2 as shown in Figure 3.2 and the probability of error can be derived just by switching the h_1A_1 with h_2A_2. Therefore the probability of error for the system is

$$P(error|h_1,h_2) = Q(\frac{h_1A_1}{\sigma_N}) + \frac{1}{2}[Q(\frac{2h_2A_2 - h_1A_1}{\sigma_N}) - Q(\frac{2h_2A_2 + h_1A_1}{\sigma_N})] \quad (3.7)$$

$$[h_2A_2 > h_1A_1]$$

3.2.2 Probability of Error with Variable Threshold

In the previous section, we confined the thresholds to be the maximum of the individual received amplitudes at the relay. This results in the significant changes in transmit amplitudes at the terminals with epsilon changes in the channel parameters in the co-channel dependent power control algorithm which will be explained in detail in further sections of this section. Now, let us consider the threshold to be a varying threshold as shown in Figure 3.3 and solve for the probability of error.

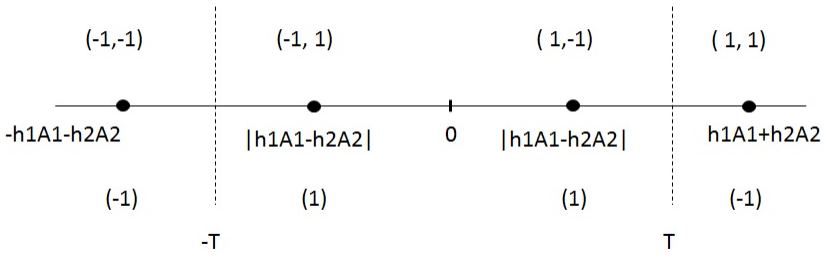

Figure 3.3: Variable threshold model

The general probability of error mentioned in the equation 3.2 prevails even for this case. Let us solve the individual terms of the equation. With a variable threshold T, the first term will be

$$P(error|1sent) = Q(\frac{T + h_1A_1 - h_2A_2}{\sigma_N}) + Q(\frac{T - h_1A_1 + h_2A_2}{\sigma_N}) \qquad (3.8)$$

then, the second term will be

$$P(error|0sent) = 1 - Q(\frac{T + h_1A_1 + h_2A_2}{\sigma_N}) + Q(\frac{T - h_1A_1 - h_2A_2}{\sigma_N}) \tag{3.9}$$

Substituting the above two equations in the equation 3.2, we arrive at the probability of error equation for the variable threshold system model.

$$\begin{aligned} P(error|h_1, h_2) = \frac{1}{2}[1 &+ Q(\frac{T + h_1A_1 - h_2A_2}{\sigma_N}) + Q(\frac{T - h_1A_1 + h_2A_2}{\sigma_N}) \\ &- Q(\frac{T + h_1A_1 + h_2A_2}{\sigma_N}) - Q(\frac{T - h_1A_1 - h_2A_2}{\sigma_N})] \end{aligned} \tag{3.10}$$

3.3 Optimal Power Control Functions

In this section, we will derive the Co-Channel Dependent (CCD) optimal power control functions using the probability of error equations derived in the previous section. Usually the channel inversion power control at the terminal can negate the channel influence on the transmitted symbol at the relay, but this can result in nonlinear input power variations at the terminal that can reach up to infinity, which is practically improbable and drains the transmit source energy rapidly to an extreme extent. So, to overcome such implications we provide caps on the average transmitted power from the terminals. Let us suppose if the terminals are being operated at X dB, then whatever power control made on the terminals should give us the average transmitted power as X dB.

For the rest of the work, we consider the case, where the power control at each terminal is averaged to 1. Then, the probability of error equations derived in the previous section are incorporated with $\sqrt{\frac{2E_b}{N_0}}$, which is the operating power level. We also assume

$$r_1 = \frac{A_1}{\sigma_N}$$

$$r_2 = \frac{A_2}{\sigma_N}$$

$$\begin{aligned}\therefore P(error|h_1,h_2) &= Q((h_2R_2)\sqrt{\frac{2E_{b2}}{N_0}}) \\ &+ \frac{1}{2}[Q((2h_1R_1\sqrt{\frac{2E_{b1}}{N_0}} - h_2R_2\sqrt{\frac{2E_{b2}}{N_0}})) \\ &- Q((2h_1R_1\sqrt{\frac{2E_{b1}}{N_0}} + h_2R_2\sqrt{\frac{2E_{b2}}{N_0}})] \\ &[h_1A_1 > h_2A_2]\end{aligned} \tag{3.11}$$

$$\begin{aligned}P(error|h_1,h_2) &= Q((h_1R_1)\sqrt{\frac{2E_{b1}}{N_0}}) \\ &+ \frac{1}{2}[Q((2h_2R_2\sqrt{\frac{2E_{b2}}{N_0}} - h_1R_1\sqrt{\frac{2E_{b1}}{N_0}})) \\ &- Q((2h_2R_2\sqrt{\frac{2E_{b2}}{N_0}} + h_1R_1\sqrt{\frac{2E_{b1}}{N_0}})] \\ &[h_2A_2 > h_1A_1]\end{aligned} \tag{3.12}$$

For the variable threshold T, the probability of error equation can be

$$\begin{aligned}P(error|h_1,h_2) = \frac{1}{2}[1 &+ Q(T + h_1R_1\sqrt{\frac{2E_{b1}}{N_0}} - h_2R_2\sqrt{\frac{2E_{b2}}{N_0}}) \\ &+ Q(T - h_1R_1\sqrt{\frac{2E_{b1}}{N_0}} + h_2R_2\sqrt{\frac{2E_{b2}}{N_0}}) \\ &- Q(T + h_1R_1\sqrt{\frac{2E_{b1}}{N_0}} + h_2R_2\sqrt{\frac{2E_{b2}}{N_0}}) \\ &- Q(T - h_1R_1\sqrt{\frac{2E_{b1}}{N_0}} - h_2R_2\sqrt{\frac{2E_{b2}}{N_0}})]\end{aligned} \tag{3.13}$$

where $r_1 = R_1 \times \sqrt{\frac{2E_{b1}}{N_0}}$ and $r_2 = R_2 \times \sqrt{\frac{2E_{b2}}{N_0}}$

3.3.1 CCD Power Control for Fixed Threshold

Let us assume that the terminals operate at equal dB levels. So, the terms in the probability of error equations

$$\sqrt{\frac{2E_{b1}}{N_0}} = \sqrt{\frac{2E_{b2}}{N_0}} = \sqrt{\frac{2E_b}{N_0}}$$

Let us also assume the received amplitudes from terminals 1 and 2 at the relay are "a" and "b" respectively. $\therefore h_1R_1 = a$ and $h_2R_2 = b$. So, the probability of error in equations 3.13 and 3.14 are modified to

$$\begin{aligned} \therefore P(error|h_1,h_2) = Q((b)\sqrt{\frac{2E_b}{N_0}}) + \frac{1}{2}[Q((2a-b)\sqrt{\frac{2E_b}{N_0}}) \\ - Q((2a+b)\sqrt{\frac{2E_b}{N_0}}] \end{aligned} \tag{3.14}$$

$$[a > b]$$

$$\begin{aligned} P(error|h_1,h_2) = Q((a)\sqrt{\frac{2E_b}{N_0}}) + \frac{1}{2}[Q((2b-a)\sqrt{\frac{2E_b}{N_0}}) \\ - Q((2b+a)\sqrt{\frac{2E_b}{N_0}})] \end{aligned} \tag{3.15}$$

$$[b > a]$$

The main motto here is to minimize the probability of error equation for this fixed threshold i.e maximum of either of the received amplitudes, system with constraints on the total average controlled power of each individual terminal to be equal to 1. The total average probability of error for the system is given as:

$$P(error) = \iint P(error|h_1,h_2)f(h_1,h_2)dh_1dh_2 \tag{3.16}$$

So the minimization function will be

$$\text{Minimize} \iint P(error|h_1, h_2) f(h_1, h_2) dh_1 dh_2 \tag{3.17}$$

$$\text{Subject to} \iint R_1^2 f(h_1, h_2) dh_1 dh_2 = 1$$

$$\iint R_2^2 f(h_1, h_2) dh_1 dh_2 = 1$$

Using Lagrangian minimization techniques, we arrive at the following minimization function:

$$\iint [P(error|h_1, h_2) + \mu_1 R_1^2 + \mu_2 R_2^2 - \mu_1 - \mu_2] f(h_1, h_2) dh_1 dh_2 \tag{3.18}$$

To minimize the above double integral expression we can minimize it at each and every instant of h_1 and h_2. So our minimization function with R_1 and R_2 as variables is as follows

$$L = P(error|h_1, h_2) + \mu_1 R_1^2 + \mu_2 R_2^2 \tag{3.19}$$

Writing the above minimization function in terms of "a" and "b", we have

$$L = P(error|a, b) + w_1 a^2 + w_2 b^2 \tag{3.20}$$

$$\text{where } w_1 = \frac{\mu_1}{h_1^2} \text{ and } w_2 = \frac{\mu_2}{h_2^2}$$

From the above equation find a,b for each (w_1,w_2) pair that minimizes L. These optimal a and b values for each pair of (w_1,w_2) are used to find the Lagrangian multipliers μ_1 and μ_2 which are constant for particular operating dB level of the

terminals. The equation

$$\iint R_i^2 f(h_1, h_2) dh_1 dh_2 = 1 \tag{3.21}$$

where $i = [1, 2]$, is used to evaluate the Lagrange multipliers, since R_i is a function of these Lagrange multipliers μ_1 and μ_2. $f(h_1, h_2)$ can be written as $f(h_1)f(h_2)$ as both the channel gains are mutually independent Rayleigh random variables. Using the density functions of the Rayleigh random variables in the equation 3.21, we arrive at the following equations which are used to solve for the μ_1 and μ_2 where the optimal a and b are calculated for each h_1 and h_2.

$$4 \iint a^2 \frac{h_2}{h_1} e^{-(h_1^2+h_2^2)} dh_1 dh_2 = 1 \tag{3.22}$$

$$4 \iint b^2 \frac{h_1}{h_2} e^{-(h_1^2+h_2^2)} dh_1 dh_2 = 1 \tag{3.23}$$

The Lagrange multiplier μ_1 and μ_2 values at particular dB level for this fixed threshold system are as shown in the Table 3.2.

Using these Lagrangian values we can calculate the transmit amplitudes R_1 and R_2 from the terminals as a function of h_1 and h_2 as shown in the Figures 3.4 and 3.5.

From the Figures 3.4 and 3.5, we can observe that at some particular combinations of h_1 and h_2, there is a substantial change in the transmit amplitudes with epsilon change in the channel parameters. This is due to the confinement of thresholds to the maximum of the received independent amplitudes at the relay. This can be controlled by using a variable threshold between the symbols in signal constellation, which is a function of the received independent amplitudes a and b. In the next subsection, we will see the behaviour of the variable threshold system along with

Table 3.2: Lagrange multiplier values for fixed threshold case

SNR in dB	μ_1	μ_2
0	0.059	0.059
1	0.0585	0.0585
2	0.0572	0.0572
3	0.054	0.054
4	0.05	0.05
5	0.045	0.045
6	0.039	0.039
7	0.0325	0.0325
8	0.026	0.026
9	0.02	0.02
10	0.0145	0.0145
11	0.0105	0.0105
12	0.0063	0.0063
13	0.0037	0.0037
14	0.0018	0.0018
15	0.00075	0.00075

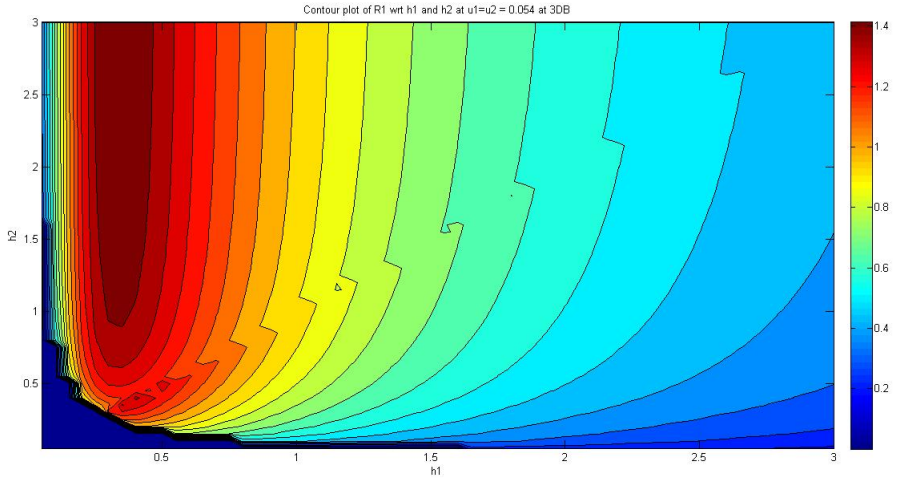

Figure 3.4: R_1 as a function of h_1 and h_2 at 3dB for fixed threshold

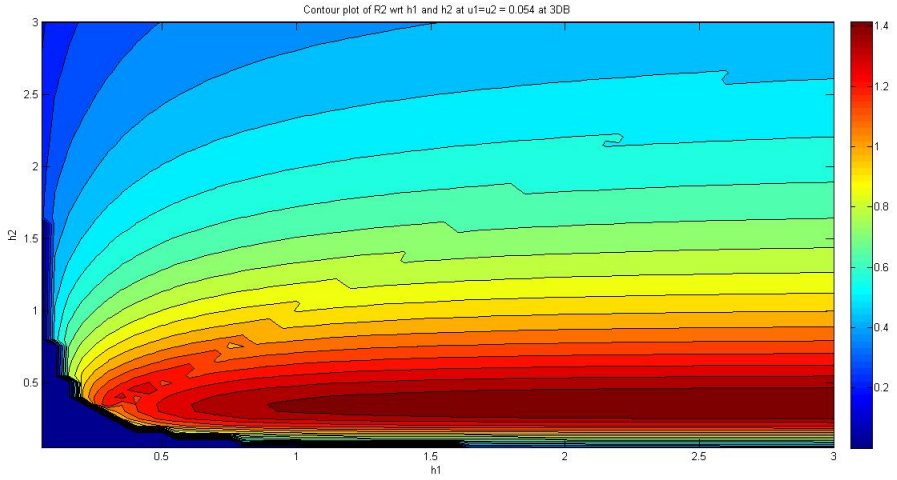

Figure 3.5: R_2 as a function of h_1 and h_2 at 3dB for fixed threshold

the transmit amplitude functions. The probability error curve at the relay with the CCD-Fixed threshold algorithm implemented at the terminals for different average SNR levels is as shown in the Figure 3.6

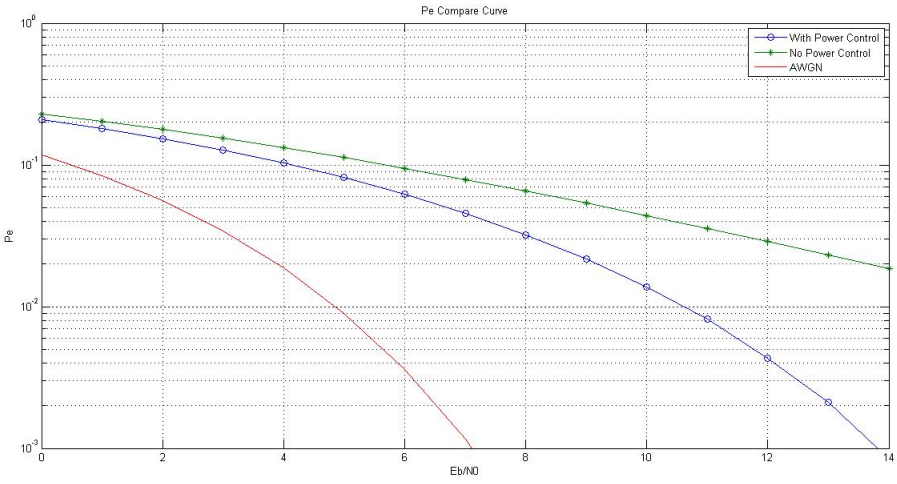

Figure 3.6: Performance comparison using probability of error curves for AWGN, with power control and without power control for CCD-fixed threshold system

3.3.2 CCD Power Control for Variable Threshold

The system model for a variable threshold is as shown in Figure 2.2. With the threshold T as a function of the received amplitudes, assuming $h_1R_1 = a$, $h_2R_2 = b$ and the terminals to be operating at equal SNR levels, the probability of error equation given for the system in the equation 3.15 can be written as

$$\begin{aligned} P(error|h_1,h_2) = \frac{1}{2}[1 &+ Q((T + h_1R_1 - h_2R_2)\sqrt{\frac{2E_b}{N_0}}) \\ &+ Q((T - h_1R_1 + h_2R_2)\sqrt{\frac{2E_b}{N_0}}) \\ &- Q((T + h_1R_1 + h_2R_2)\sqrt{\frac{2E_b}{N_0}}) \\ &- Q((T - h_1R_1 - h_2R_2)\sqrt{\frac{2E_b}{N_0}})] \end{aligned} \tag{3.24}$$

The total average probability of error for the system is given as:

$$P(error) = \iint P(error|h_1,h_2)f(h_1,h_2)dh_1dh_2 \tag{3.25}$$

So the minimization function will be

$$\text{Minimize} \iint P(error|h_1,h_2)f(h_1,h_2)dh_1dh_2 \tag{3.26}$$

$$\text{Subject to} \iint R_1^2 f(h_1,h_2)dh_1dh_2 = 1$$

$$\iint R_2^2 f(h_1,h_2)dh_1dh_2 = 1$$

Using the Lagrangian minimization techniques, we arrive at the following minimization function:

$$\iint [P(error|h_1, h_2) + \mu_1 R_1^2 + \mu_2 R_2^2 - \mu_1 - \mu_2] f(h_1, h_2) dh_1 dh_2 \tag{3.27}$$

To minimize the above double integral expression we can minimize it at each and every instant of h_1 and h_2. So our minimization function with R_1 and R_2 as variables is as follows

$$L = P(error|h_1, h_2) + \mu_1 R_1^2 + \mu_2 R_2^2 \tag{3.28}$$

Writing the above minimization function in terms of "a" and "b", we have

$$L = P(error|a, b) + w_1 a^2 + w_2 b^2 \tag{3.29}$$

$$\text{where } w_1 = \frac{\mu_1}{h_1^2} \text{ and } w_2 = \frac{\mu_2}{h_2^2}$$

Using the Newton Raphson method to find the optimal threshold value as a function of the a and b, it takes just 3-5 iterations to converge. This optimal threshold is used to estimate the optimal values of a and b for each (w_1,w_2) pair that minimizes L. These optimal a and b values for each pair of (w_1,w_2) are used to find the Lagrangian multipliers μ_1 and μ_2 which are constant for particular operating dB level of the terminals. The equation

$$\iint R_i^2 f(h_1, h_2) dh_1 dh_2 = 1 \tag{3.30}$$

where $i = [1, 2]$, is used to evaluate the Lagrange multipliers, since R_i is a function of these Lagrange multipliers μ_1 and μ_2. $f(h_1, h_2)$ can be written as $f(h_1)f(h_2)$ as both the channel gains are mutually independent Rayleigh random variables. Using

the distribution functions of the Rayleigh random variables in the equation 3.23, the following equations are used to solve for the μ_1 and μ_2 using Riemann sum method where the optimal a and b are calculated for each h_1 and h_2.

$$4 \iint a^2 \frac{h_2}{h_1} e^{-(h_1^2+h_2^2)} dh_1 dh_2 = 1 \tag{3.31}$$

$$4 \iint b^2 \frac{h_1}{h_2} e^{-(h_1^2+h_2^2)} dh_1 dh_2 = 1 \tag{3.32}$$

The Lagrange multiplier μ_1 and μ_2 values at particular dB level for this fixed threshold system are as shown in the Table 3.3. Using these Lagrangian values we can

Table 3.3: Lagrange multiplier values for variable threshold case

SNR in dB	μ_1	μ_2
0	0.058	0.058
1	0.0575	0.0575
2	0.0562	0.0562
3	0.053	0.053
4	0.049	0.049
5	0.044	0.044
6	0.038	0.038
7	0.032	0.032
8	0.0255	0.0255
9	0.0195	0.0195
10	0.0144	0.0144
11	0.01	0.01
12	0.0063	0.0063
13	0.00365	0.00365
14	0.0018	0.0018
15	0.00075	0.00075

calculate the transmit amplitudes R_1 and R_2 from the terminals along with the optimal threshold as a function of h_1 and h_2 as shown in the Figures 3.7, 3.8 and 3.9.

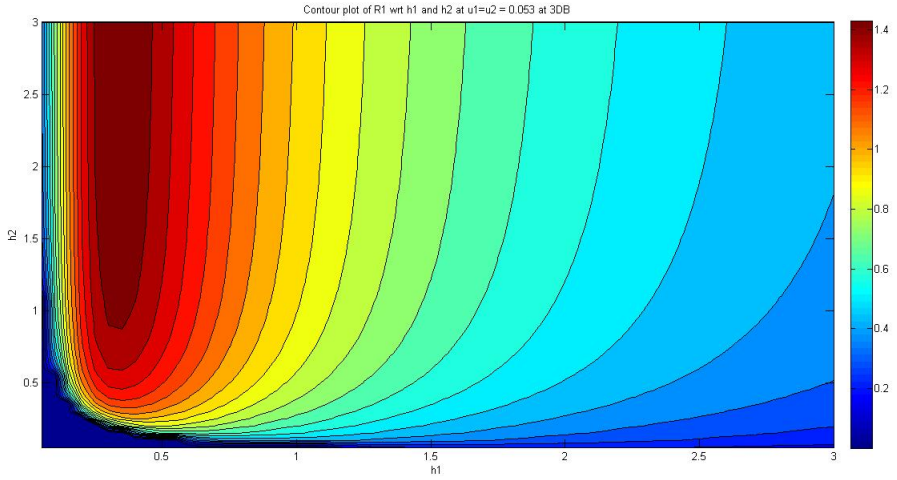

Figure 3.7: R_1 as a function of h_1 and h_2 at 3dB for variable threshold

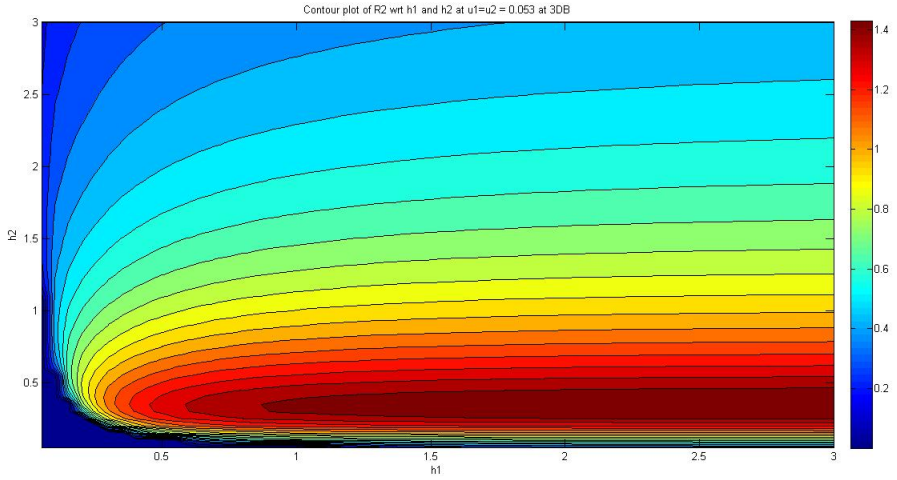

Figure 3.8: R_2 as a function of h_1 and h_2 at 3 dB for variable threshold

The probability error curve at the relay with the CCD-Variable threshold algorithm implemented at the terminals for different average SNR levels is as shown in the Figure 3.10

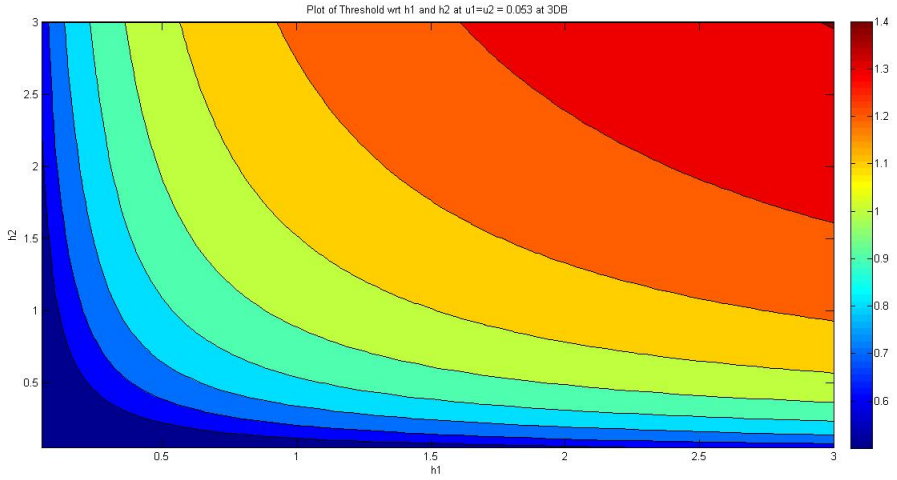

Figure 3.9: Optimal threshold as a function of h_1 and h_2 at 3 dB for variable threshold

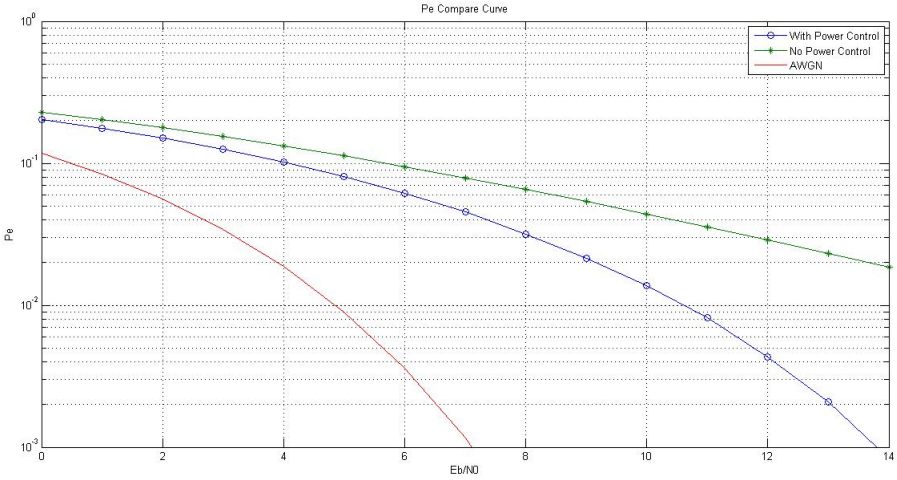

Figure 3.10: Performance comparison using probability of error curves for AWGN, with power control and without power control for CCD-variable threshold system

3.3.3 Sub-optimal Co-Channel Independent (CCI) Power Control Function

In this section, we will derive the closed form optimal power control function for the single channel user system as shown in Figure 2.3 operating with an underlying

BPSK modulation. We then extend this single channel power control to our system model by applying the power control independently on each of the terminals and measure the performance of the system.

Let us consider h as a channel parameter between the terminal and the receiver and A be the amplitude control function at the terminal. Then the probability of error for the system is given by

$$P(error|h) = Q(\frac{h_1 A_1}{\sigma_N}) \tag{3.33}$$

The average probability error of the system is given by

$$P(error) = \int P(error|h) f(h) dh \tag{3.34}$$

Let us assume $r = \frac{A}{\sigma_N}$ and as shown in the previous section , we can write $r = R \times \sqrt{\frac{2E_b}{N_0}}$, where R is an amplitude control function of channel parameter . The amplitude control function R when averaged over the probability density function of channel parameters, will be equal to 1. With the above assumptions the probability of error equation that should be minimized to achieve the optimal performance is given below

$$P(error) = \int Q(hR\sqrt{\frac{2E_b}{N_0}}) f(h) dh \tag{3.35}$$

$$\text{subject to} \int R^2 f(h) dh = 1$$

Using Lagrange minimization technique the expression that needs to be minimized is

$$\int [Q(hR\sqrt{\frac{2E_b}{N_0}}) + \mu R^2 - \mu] f(h) dh \tag{3.36}$$

As we know that the above expression can be minimum when it is minimum at each

and every instant of h with R as a variable. So, now the equation we end up for minimizing is

$$L = Q(hR\sqrt{\frac{2E_b}{N_0}}) + \mu R^2 \tag{3.37}$$

Taking the partial derivative with respect to R we have

$$\frac{\partial L}{\partial R} = \frac{-h}{\sqrt{2\pi}}\sqrt{\frac{2E_b}{N_0}}e^{-h^2R^2\frac{E_b}{N_0}} + 2\mu R \tag{3.38}$$

Equating the above equation to zero, we arrive at an equation for R given as

$$R = \frac{0.707107\sqrt{W(\frac{0.159155(\frac{E_b}{N_0})^2h^4}{\mu^2})}}{h\sqrt{\frac{E_b}{N_0}}} \tag{3.39}$$

where W is the Lambert W function. The Lagrange multiplier μ can be evaluated by using the constraint mentioned in the minimization equation. Substituting the pdf function of Rayleigh random variable in the constraint function, the equation used to solve for the μ is given by

$$2\int R^2 h e^{-h^2} dh = 1 \tag{3.40}$$

Using Riemann sum method and making the average to be equal to 1 for the above equation, the Lagrange multiplier values at each SNR level are given in the Table 3.4 The probability of error curve at the relay for a single channel user system with the optimal power control algorithm implemented at the terminals for different average SNR levels is as shown in the Figure 3.11. The amplitude control function at the terminal as a function of the channel parameter h is as shown in the Figure 3.12.

Table 3.4: Lagrange multiplier values for single user system

SNR in dB	μ_1
0	0.0914
1	0.08775
2	0.08259
3	0.076
4	0.0682
5	0.0596
6	0.0505
7	0.0412
8	0.0324
9	0.0243
10	0.01735
11	0.01175
12	0.00743
13	0.00425
14	0.0021
15	0.000855

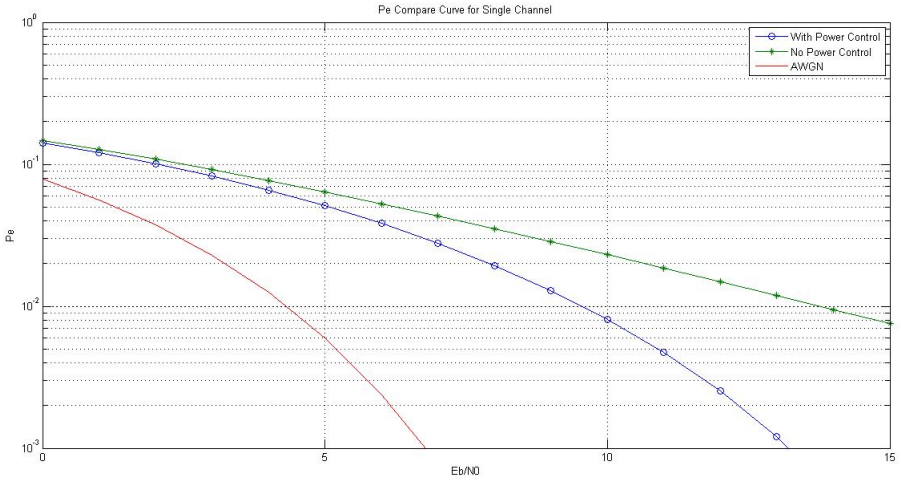

Figure 3.11: Performance comparison using probability of error curves for AWGN, with power control and without power control for single user system

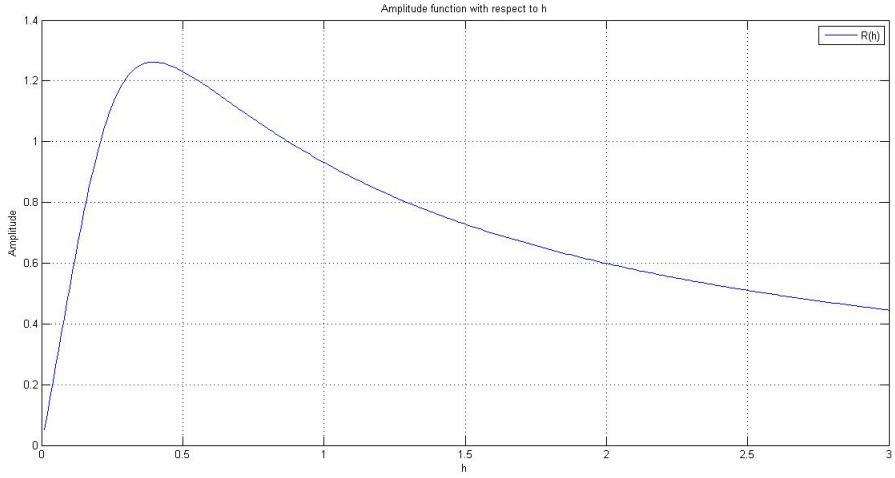

Figure 3.12: Amplitude function as a function of channel parameter H

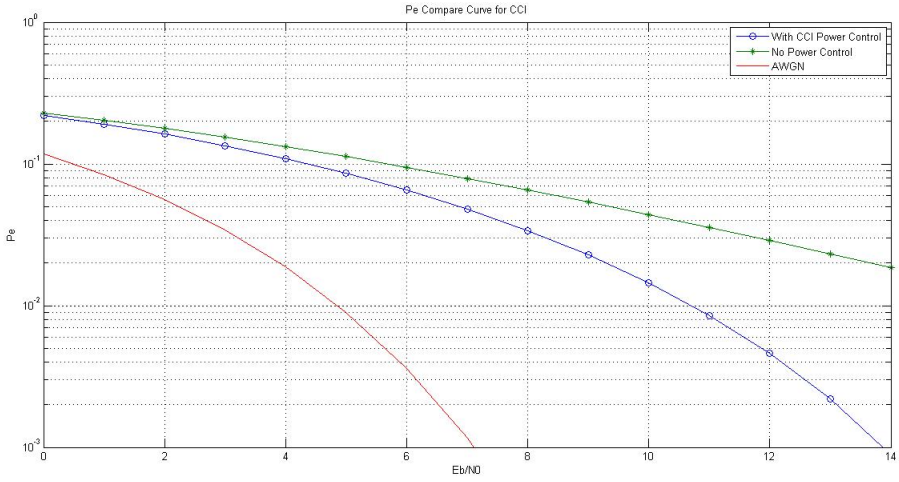

Figure 3.13: Probability of error curve for CCI model

Now, we extend this single channel optimal power control to our two way relay system model by implementing the optimal power control algorithm on the terminals independently. We call this model of implementation as CCI optimal power control algorithm as the power control on the terminals is independent of the other terminals

channel parameters. The performance at the relay node with CCI power control algorithm is as shown in the Figure 3.13 and the amplitude function at the each terminal is similar to the one shown in Figure 3.12.

4. COMPARISONS, CONCLUSIONS AND FUTURE WORK

In this section we will compare the results of the proposed optimal power control algorithms and derive the conclusions for this thesis work. We then identify possible future work as an extension to the conclusions.

4.1 Comparisons and Conclusions

In this section, first we will compare the performances of optimal CCD power control algorithm and sub-optimal CCI power control algorithm derived in the section 3 and then we will compare these results with the previous power control algorithms or techniques mentioned in section2.

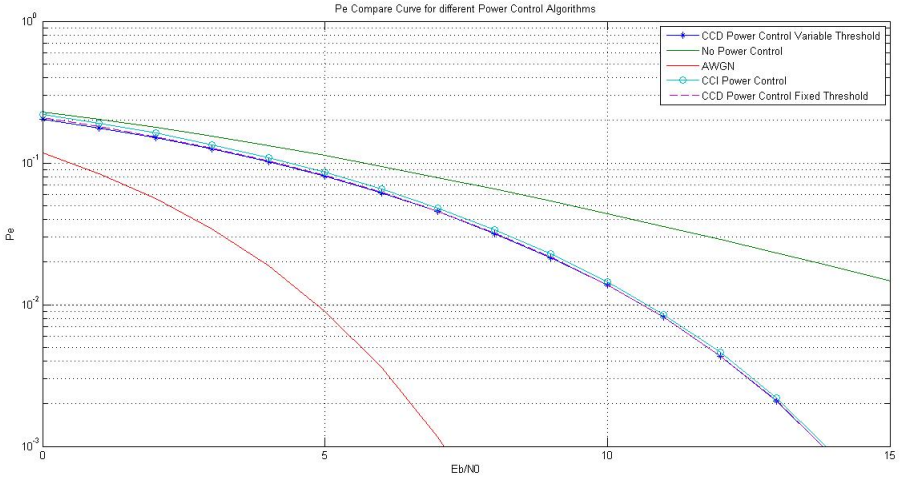

Figure 4.1: Performance comparison at the relay for different power control algorithms in our thesis

From the Figure 4.1, we can see that performance of the CCD optimal power control algorithm with fixed threshold is similar to the performance of CCD optimal

power control algorithm with variable threshold system model. The only difference with these algorithms is that variable threshold model eliminates the irregularities in the amplitude function that arose due to confining of the thresholds to the maximum of the received amplitudes. We can also observe that the performance of CCI sub-optimal power control algorithm system model is almost similar to the CCD power control performance with only subtle degradation in performance. From this, we can draw a strong conclusion that the co-channel state information is not mandatory at the terminals to achieve better performance as we can neglect the subtle degradation in performance of the system at the relay. This reduces the complexity of the system implementation.

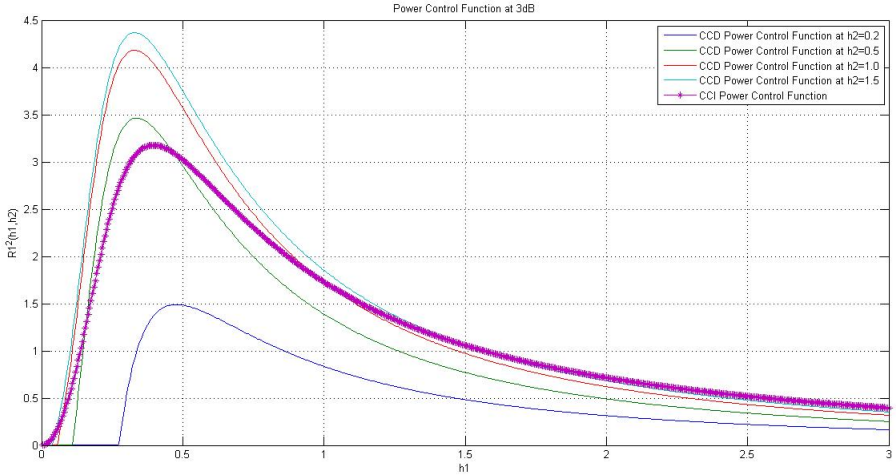

Figure 4.2: Power control function comparison for CCD and CCI algorithms

By observing the power control functions of CCD and CCI systems as shown in the Figure 4.2, we can conclude that the perfect estimation of channel parameters and amplitude calculation is not mandatory to achieve near optimal performance at

the relay. From the Figure 4.3, we can see that the optimal CCD and the sub-optimal CCI power control algorithms achieve a huge performance improvement as compared to the power control algorithms described in section 2.

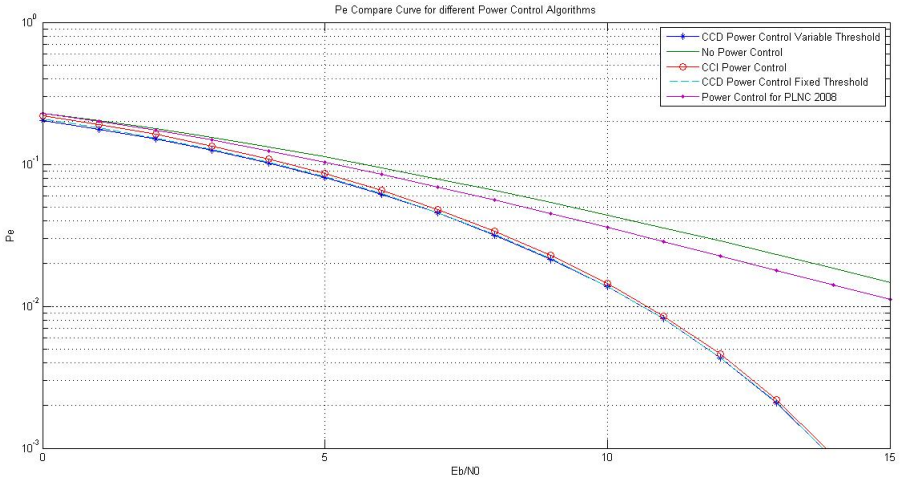

Figure 4.3: Performance comparison for CCD and CCI algorithms with power control algorithm in 2008 paper

By observing the set of Figures in 4.4 which shows the instantaneous received amplitudes at the relay from terminals 1 and 2 for CCD Fixed Threshold, CCD Variable Threshold and CCI algorithms, we can conclude and postulate that the common paradigm of equal received amplitudes at the relay for optimal performance in TWRN implementing PLNC is wrong. We can say the assumption of equal received amplitudes at the relay as in CDMA power control to alienate the near far effect is not appropriate in PLNC systems.

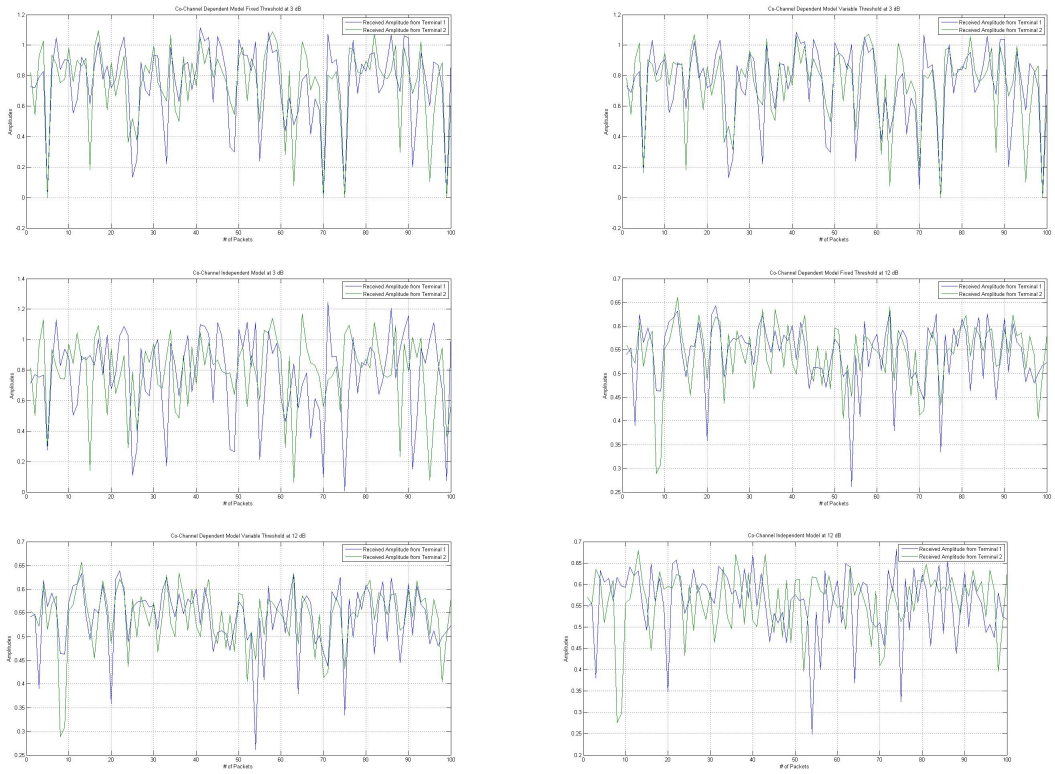

Figure 4.4: Instantaneous received amplitudes at the relay for 3dB and 12dB with CCD and CCI algorithms at the terminals

4.2 Future Work

From the conclusions we have arrived at in this thesis, we can extend this work to

- A higher modulation format such as QAM and test the performance of the system for the proposed CCD and CCI power control algorithms.
- Feedback implementation, where quantized channel state information is feedback to the terminal and performance of the system is evaluated with the variable quantization bits.

REFERENCES

[1] S. Abdallah and I.N. Psaromiligkos. Blind channel estimation for amplify-and-forward two-way relay networks employing m-psk modulation. *Signal Processing, IEEE Transactions*, 60(7):3604–3615, July 2012.

[2] J. Hayes. Adaptive feedback communications. *Communication Technology, IEEE Transactions*, 16(1):29–34, February 1968.

[3] M. Jain, S.L. Miller, and A. Sprintson. Parameter estimation and tracking in physical layer network coding. In *Global Telecommunications Conference (GLOBECOM 2011), 2011 IEEE*, pages 1–6, Dec 2011.

[4] S. Katti, S. Gollakota, and D. Katabi. Embracing wireless interference: Analog network coding. *Proceedings of the 2007 conference on Applications, technologies, architectures, and protocols for computer communications (SIGCOMM-07)*, pp. 397-408, Aug. 2007.

[5] S. Katti, H. Rahul, Wenjun Hu, D. Katabi, M. Medard, and J. Crowcroft. Xors in the air: Practical wireless network coding. *Networking, IEEE/ACM Transactions*, 16(3):497–510, June 2008.

[6] T. Koike-Akino, P. Popovski, and Vahid Tarokh. Optimized constellations for two-way wireless relaying with physical network coding. *Selected Areas in Communications, IEEE Journal*, 27(5):773–787, June 2009.

[7] Yixin Li and Fu-Chun Zheng. Limited feedback power control for physical layer network coding via power ratio quantization. In *Vehicular Technology Conference (VTC Fall), 2013 IEEE 78th*, pages 1–5, Sept 2013.

[8] Lu Lu, Soung Chang Liew, and Shengli Zhang. Optimal decoding algorithm for asynchronous physical-layer network coding. In *Communications (ICC), 2011 IEEE International Conference*, pages 1–6, June 2011.

[9] S.L. Miller. Detection of imperfectly synchronized data streams in physical layer network coding. In *Global Communications Conference (GLOBECOM), 2014 IEEE*, pages 1577–1582, Dec 2014.

[10] Wooseok Nam, Sae-Young Chung, and Yong H. Lee. Capacity of the gaussian two-way relay channel to within 1/2 bit. *Information Theory, IEEE Transactions*, 56(11):5488–5494, Nov 2010.

[11] M. Noori and M. Ardakani. On symbol mapping for binary physical-layer network coding with psk modulation. *Wireless Communications, IEEE Transactions*, 11(1):21–26, January 2012.

[12] E.C.Y. Peh, Ying-Chang Liang, and Yong Liang Guan. Power control for physical-layer network coding in fading environments. In *Personal, Indoor and Mobile Radio Communications, 2008. PIMRC 2008. IEEE 19th International Symposium*, pages 1–5, Sept 2008.

[13] Shiqiang Wang, Qingyang Song, Lei Guo, and A. Jamalipour. Constellation mapping for physical-layer network coding with m-qam modulation. In *Global Communications Conference (GLOBECOM), 2012 IEEE*, pages 4429–4434, Dec 2012.

[14] M.P. Wilson, K. Narayanan, H.D. Pfister, and A. Sprintson. Joint physical layer coding and network coding for bidirectional relaying. *Information Theory, IEEE Transactions*, 56(11):5641–5654, Nov 2010.

[15] Y. Wu, P. Chou, and S. Kung. Information exchange in wireless networks with network coding and physical-layer broadcast. *Conference on Information Sciences and Systems*, Mar. 2005.

[16] Hyun Jong Yang, Youngchol Choi, and Joohwan Chun. Modified high-order pams for binary coded physical-layer network coding. *Communications Letters, IEEE*, 14(8):689–691, August 2010.

[17] Tao Yang and I.B. Collings. Asymptotically optimal error-rate performance of linear physical-layer network coding in rayleigh fading two-way relay channels. *Communications Letters, IEEE*, 16(7):1068–1071, July 2012.

[18] S. Zhang, S. Liew, and P.Lam. Physical layer network coding. *Proc. 12th Annual International Conference on Mobile Computing and Networking (ACM MobiCom 2006)*, Sep. 2006.

[19] Shengli Zhang, Soung-Chang Liew, and P.P. Lam. On the synchronization of physical-layer network coding. In *Information Theory Workshop, 2006. ITW '06 Punta del Este. IEEE*, pages 404–408, Oct 2006.

[20] Qiong Zhao, Zhendong Zhou, Jun Li, and B. Vucetic. Joint semi-blind channel estimation and synchronization in two-way relay networks. *Vehicular Technology, IEEE Transactions*, 63(7):3276–3293, Sept 2014.